*Polish Journal of Chemical Technology, 16, **4**, 95 — 100, 10.2478/pjct-2014-0076*

Impact of heating rate and solvent on Ni-based catalysts prepared by solution combustion method for syngas methanation

Yan Zeng, Hongfang Ma, Haitao Zhang, Weiyong Ying*, Dingye Fang

East China University of Science and Technology, Engineering Research Center of Large Scale Reactor Engineering and Technology, Ministry of Education, State Key Laboratory of Chemical Engineering, Shanghai, China 200237
**Corresponding author: e-mail: wying@ecust.edu.cn*

Ni-Al_2O_3 catalysts prepared by solution combustion method for syngas methanation were enhanced by employing various heating rate and different solvent. The catalytic properties were tested in syngas methanation. The result indicates that both of heating rate and solvent remarkably affect Ni particle size, which is a key factor to the catalytic activity of Ni-Al_2O_3 catalysts for syngas methanation. Moreover, the relationship between Ni particle size and the production rate of methane per unit mass was correlated. The optimal Ni-Al_2O_3 catalyst prepared in ethanol at 2°C/min, achieves a maximum production rate of methane at the mean size of 20.8 nm.

Keywords: nickel catalysts, syngas methanation, solution combustion method.

INTRODUCTION

Natural gas has been considered as a promising energy source because of its clean nature, high calorific value and easiness for complete combustion. However, due to its poor reserves in some regions of the world, synthetic natural gas (SNG) plays an important role as an alternative energy[1, 2]. Therefore, syngas methanation as a useful technology to synthesize natural gas, has attracted much attention from both academia and industry[3, 4] ($CO + 3H_2 \rightarrow CH_4 + H_2O$, $\Delta H_{298K} = -206.1$ kJ · mol^{-1}; $CO_2 + 4H_2 \rightarrow CH_4 + 2H_2O$, $\Delta H_{298K} = -165.0$ kJ · mol^{-1}). Since Sabatier and Senderens discovered that some metals such as Ni, Ru, Rh, Pt, Fe, and Co possessed a good catalytic activity for syngas methanation in 1902[5], methanation catalysts integrating active metal had been developed well. Ru-based catalysts retain the best active for syngas methanation, but limited resource and high cost restrict their large-scale commercialization[6–8]. Ni-based catalysts have been widely used for their low cost, high catalytic activity and selectivity for methane[9–11]. In recent decades, great efforts have been made to produce high-efficiency catalysts retaining high activity at low-temperature (ca. 300°C) and high stability at high-temperature (ca. 600°C). Since Ni-based catalysts prepared by conventional methods (coprecipitation, impregnation, sol-gel and mechanical mixing) possess low activity at low-temperature, and deactivate easily at high-temperature, Zhao et al. employed solution combustion method (SCM) to synthesize Ni-based catalysts for CO methanation[12], which shows excellent catalytic activity and stability. The aim of our work is to further improve and optimize the SCM by investigating the condition of preparation process.

In this work, we employ various heating rate (2°C · min^{-1}, 5°C · min^{-1} and 10°C · min^{-1}) and different solvent (ethanol, n-propanol and glycerol) to prepare Ni-Al_2O_3 catalysts by SCM. The as-synthesized catalysts were characterized by N_2 adsorption-desorption, XRD, H_2-TPR and TEM. Effects of heating rate and solvent on CO conversion and stability, as well as the relationship between Ni particle size and production rate of methane per unit mass of Ni were studied.

EXPERIMENTAL

Catalyst preparation

$Ni(NO_3)_2 \cdot 6H_2O$ and $Al(NO_3)_3 \cdot 9H_2O$ were used as metal precursor salts. Ethanol, n-propanol and glycerol were used as the solvent and fuel. Typically, 14.87 g $Ni(NO_3)_2 \cdot 6H_2O$ and 51.52 g $Al(NO_3)_3 \cdot 9H_2O$ were dissolved in 200 mL ethanol at room temperature, while the same amount of metal precursor salts were dissolved in 200 mL n-propanol and glycerol respectively, which were preheated in water bath at 70°C. These mixtures were vigorously stirred until Ni and Al salts completely dissolved, and then kept at 70°C for 6 h to ensure these solutions at the same initial temperature. After that, these stable and clear solutions were heated from 70 to 700°C under static air in a muffle furnace with given heating rate (combustion occurred spontaneously during the heating process), and then kept at 700°C for 7 h. The prepared Ni-Al_2O_3 catalysts were denoted as 30Ni-XY, where 30 showed Ni weight content in the catalyst, X represented the heating rate (°C · min^{-1}) and Y indicated the type of solvent (E = ethanol, P = n-propanol and G = glycerol). For comparison, pure Al_2O_3 was also prepared at 2°C · min^{-1} using ethanol as solvent.

Catalyst characterization

Nitrogen adsorption-desorption isotherms were obtained with Micrometrics ASAP 2020 apparatus. Prior to N_2 adsorption, the samples were degassed under vacuum at 200°C for 4 h. Specific surface areas were measured by Brunauer Emmet Teller (BET) method. Total pore volume and pore sizes were evaluated using the standard Barrett-Joyner-Halenda (BJH) treatment.

Powder X-ray diffraction (XRD) patterns were recorded on a Rigaku D/Max 2550 using Cu Kαradiation at 40kV and 100mA. XRD patterns were determined over a 2θ range of 10–80° and a step size of 0.02°.

Hydrogen temperature programmed reduction (H_2--TPR) measurements were carried out on AutoChem II 2920 (Micrometrics) instrument. Prior to the H_2-TPR measurements, 200 mg sample placed in a quartz U-tube reactor was pretreated in Ar stream at 500°C for 0.5 h and then cooled to 50°C. H_2-TPR process was

then conducted with a gas mixture of 10 vol.% H_2 in Ar at the flow rate of 50 mL · min^{-1}, and temperature was raised from 50 to 1000°C with the heating rate of 10°C · min^{-1}. Hydrogen consumption was monitored by thermal conductivity detector (TCD).

Transmission electron microscope (TEM) images were taken by means of a JEM-1400 apparatus operated at 100 kV. In order to obtain the suitable samples, the metal oxides catalysts were reduced to the metallic state in H_2 atmosphere (100 mL · min^{-1}) for 3 h at 700°C, and cooled to room temperature in N_2 flow, then passivated in O_2/N_2 mixture (1 vol.% O_2, 100 mL · min^{-1}) for 2 h to avoid bulk oxidation of Ni nanoparticles[6]. After that, the reduced Ni-based catalysts were dispersed in ethanol by ultrasonic, and the suspension was then dropped onto a holey carbon-coated copper grid.

Syngas methanation

Syngas (carbon oxides and hydrogen) methanation reaction was carried out in a fixed-bed reactor (Φ14 × 2 × 500 mm). Inert Al_2O_3 was added at both ends of the uniform temperature zone to keep the catalyst in the middle. Typically 500 mg catalyst was used, and the total gas flow rate was 100 mL · min^{-1}, corresponding to a weight hourly space velocity (WHSV) of 12 000 mL · g^{-1} · h^{-1}. The catalyst was heated from ambient temperature to 700°C in nitrogen flow within 300 min and reduced by pure hydrogen for 3 h. Afterwards, the catalyst was cooled to reaction temperature under nitrogen flow, and then the reaction was initiated as the gas flow switched to the syngas (17.3 vol.% CO, 9.5 vol.% CO_2, 67.7 vol.% H_2, 5.5 vol.% N_2) to investigate the low-temperature catalytic activity of Ni-based catalysts at 260–340°C, 0.1 MPa and 12 000 mL · g^{-1} · h^{-1}. High-temperature stability test of 30Ni-Al_2O_3 was conducted at 600°C, 2 MPa, 12 000 mL · g^{-1} · h^{-1} and with 30 mol% water. Here, we define:

$$\text{CO conversion: } X_{CO}(\%) = \frac{N_{CO,in} - N_{CO,out}}{N_{CO,in}} \times 100 \quad (1)$$

$$\text{CO}_2\text{ conversion: } X_{CO_2}(\%) = \frac{N_{CO_2,in} - N_{CO_2,out}}{N_{CO_2,in}} \times 100 \quad (2)$$

CH_4 selectivity:

$$S_{CH_4}(\%) = \frac{N_{CH_4,out}}{(N_{CO,in} - N_{CO,out}) + (N_{CO_2,in} - N_{CO_2,out})} \times 100 \quad (3)$$

$$\text{CH}_4\text{ formation rate: } r_{CH_4} = \frac{N_{CH_4,out}}{m_{Ni}} \quad (4)$$

N is the mole flow rate (mol · h^{-1}), and m is the weight of Ni (g).

RESULTS AND DISCUSSION

The surface area (S_{BET}), pore volume (V_P) and average pore size (D_P) of the Ni-based catalysts are summarized in Table 1. The surface area, pore volume and average pore size of the Ni-Al_2O_3 catalysts are 85.2 – 150.3 m^2 · g^{-1}, 0.165 – 0.637 cm^3 · g^{-1} and 4.3–26.8 nm, respectively. It can be found that there exist a little difference of pore volume and average pore size among the catalysts except 30Ni-2G, which obtains the highest pore volume of 0.637 cm^3 · g^{-1} and average pore size of 26.8 nm. Moreover, heating rate contributes to the surface area and pore volume little, while solvent type plays the most important role.

XRD patterns of fresh calcined Ni-Al_2O_3 catalysts as well as pure Al_2O_3 are shown in Figure 1a. For pure Al_2O_3, three board diffraction peaks of γ-Al_2O_3 (JCPDS 10-0425) are presented. For fresh calcined Ni-Al_2O_3 catalysts, the diffraction peaks at 37.3°, 43.2°, 62.9°, 75.3° and 79.4° are attributed to distinct peaks of cubic NiO (JCPDS 73-1519), and the diffraction peaks at 19.1°, 31.4°, 37.0°, 45.0°, 59.7° and 65.9° derive from distinct peaks of $NiAl_2O_4$ (JCPDS 10-0339). Moreover, the average crystal diameters of NiO are estimated from (311) plane using Scherrer equation. As shown in Table 1, the mean crystal diameter of NiO (D_{NiO}) gradually increases from 31.9 to 36.9 nm when the heating rate increases from 2 to 10°C · min^{-1}. The result can be attributed to the increase of heating rate which leads to higher flame temperature, and thereby aggravating the aggregation of Ni particles. In addition, D_{NiO} of Ni-Al_2O_3 catalysts prepared in n-propanol and glycerol is smaller than that in ethanol, which implies that solvent has an effect on Ni particle size.

XRD patterns of reduced Ni-Al_2O_3 catalysts and pure Al_2O_3 are presented in Figure 1b. The diffraction peaks at 44.3°, 51.7° and 76.1°are attributed to distinct peaks of Ni (JCPDS65-0380). As shown in Figure 1b, diffraction peaks of $NiAl_2O_4$ still exist in the reduced Ni-Al_2O_3 catalysts, which indicate that $NiAl_2O_4$ is difficult to be reduced. Furthermore, the average crystal diameter of Ni (D_{Ni}) calculated from (200) plane is in good agreement with the average crystal diameter of NiO.

TPR results of all the Ni-Al_2O_3 catalysts were shown in Figure 2, in which the various peak temperatures reveal the different interaction between nickel oxides and alumina. According to the peaks in their TPR profiles

Table 1. Surface area, pore volume, average pore diameter and NiO crystal size for fresh calcined Ni-Al_2O_3 catalysts, Ni crystal size for reduced Ni-Al_2O_3 catalysts, and production rate of methane per unit mass of nickel (rCH_4)

Catalyst	S_{BET} [m^2 · g^{-1}]	V_p[a] [cm^3 · g^{-1}]	D_p[b] [nm]	D_{NiO}[c] [nm]	D_{Ni}[c] [nm]	D_{Ni}[d] [nm]	r_{CH4} [mmol · g^{-1} · h^{-1}]
30Ni-2E	110.2	0.188	4.9	31.9	20.8	22.0	221
30Ni-5E	121.2	0.209	5.0	32.3	21.6	26.2	92
30Ni-10E	120.1	0.165	4.3	36.9	29.9	30.1	50.3
30Ni-2P	150.3	0.253	4.8	27.9	17.5	18.8	61.6
30Ni-2G	85.2	0.637	26.8	20.5	10.0	16.7	44.8

[a]BJH desorption pore volume,
[b]BJH desorption average pore diameter,
[c]Calculated from XRD using Scherrer equation,
[d]Measured by TEM photo (Ni average diameter = $\Sigma n_i d_i^3 / \Sigma n_i d_i^2$).

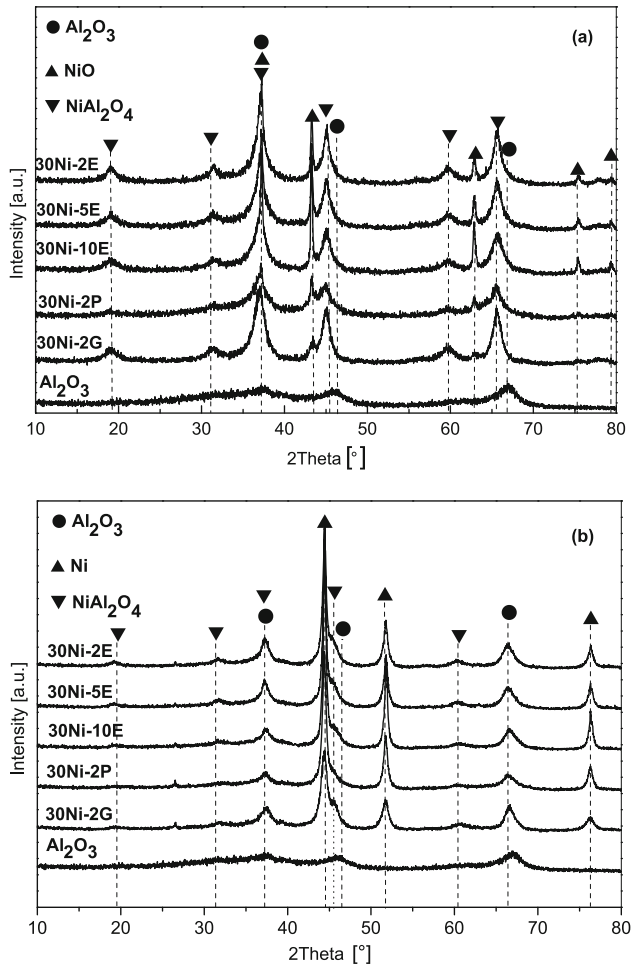

Figure 1. XRD patterns of fresh calcined Ni-Al_2O_3 catalysts (a), and reduced Ni-Al_2O_3 catalysts (b)

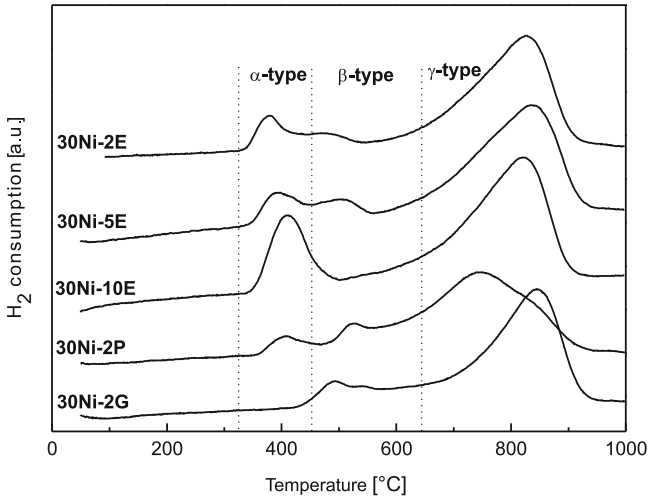

Figure 2. TPR profiles of fresh calcined Ni-Al_2O_3 catalysts

and reported in literatures [13–17], the reducible NiO species can be classified into three types: α, β and γ. The small peaks located in the low temperature region are assigned to α-type NiO species (surface amorphous NiO or bulk NiO), which are free nickel oxides species and have a weak interaction with alumina. The mild-temperature peaks represent β-type NiO species (weakly interacted with Al_2O_3 or called Ni-rich phase), which are the main sources of low-temperature activity after reduction. The high-temperature peaks are assigned to γ-type NiO species (Strongly interact or chemically bound with Al_2O_3), which are ascribed to the stable nickel aluminate phase with a spinel structure[18–20]. In the same way, the XRD patterns prove that $NiAl_2O_4$ indeed exist in the Ni--based catalysts. It should be noted that 30Ni-10E and 30Ni-2G only have two peaks. This may because that peaks of different NiO species interlap, and in some cases, α-type reduction peak would overlap with β-type. From the profiles of the catalysts prepared in ethanol, the low-temperature peaks move backward with the increase of the heating rate, and the same phenomenon is discovered in profiles of 30Ni-2P and 30Ni-2G, which shows the interaction between surface NiO and Al_2O_3 of the catalysts with higher heating rate or prepared in n-propanol and glycerol is stronger than 30Ni-2E.

TEM micrographs of reduced catalysts presented in Figure 3 clearly show that the nickel oxide particles are uniformly dispersed in the cotton-like γ-Al_2O_3. Mean particle size of Ni (D_{Ni}) determined from TEM (Nickel particles in the photo) is summarized in Table 1 (16.7–30.1 nm), and varies in line with XRD, but a little higher than those calculated using Scherrer equation from XRD. This is because TEM measures polycrystal, while XRD counts monocrystalline Ni particles. Furthermore, particle size distribution is different from average Ni particle sizes[21]. As shown in TEM and particle size distribution images, comparing with 30Ni-5E, 30Ni-10E, 30Ni-2P and 30Ni--2G, 30Ni-2E retains narrower distribution and nearer space of Ni particles that would be beneficial for the activity and stability of the catalyst on account of making good use of catalyst surface area. Gao et al.[22] found that Ni catalysts with particle size of 15–20 nm show a better performance. As shown in Figure 3f, 30Ni-2E retains a higher amount of particles between 15 and 20 nm than the other catalysts. It implies that 30Ni-2E has a higher catalytic activity. When the particle is too small or too large, it will lead to more carbon deposition and lower activity.

Figure 4a and 4b presents the catalytic activity in terms of CO and CO_2 conversion over 30Ni-2E, 30Ni-5E, 30Ni-10E, 30Ni-2P and 30Ni-2G at 0.1 MPa and 12 000 mL · g^{-1} · h^{-1} during 260–340°C. CO conversion of 30Ni-2E starts at 42.4% (260°C) and reaches nearly 100% below 320°C, which shows a better activity than our previous work. As shown in Figure 4c, 30Ni-2E also reveals a high selectivity for methane, which approaches 100% after the temperature above 300°C. The results indicate that catalytic activity decreases with the increase of heating rate, and the catalysts prepared in n-propanol and glycerol retain lower activity. As a result, it can be concluded that both heating rate and solvent play an important role in Ni particle size and distribution, affecting the catalytic activity of Ni-based catalysts for syngas methanation.

The production rate of methane per unit mass of nickel as a function of Ni crystal size was also studied at 280°C, 0.1 MPa and 12 000 mL · g^{-1} · h^{-1}. Apparently, the production rate of methane per unit mass of nickel is greatly influenced by Ni particle size, which increases with Ni crystal size to a maximum i.e., 221 mmol · g^{-1} · h^{-1} at the mean size of 20.8 nm (determined by XRD), and then declines with a further increase in size, as shown in Table 1. This phenomenon indicates that the syngas methanation over Ni-Al_2O_3 catalysts at

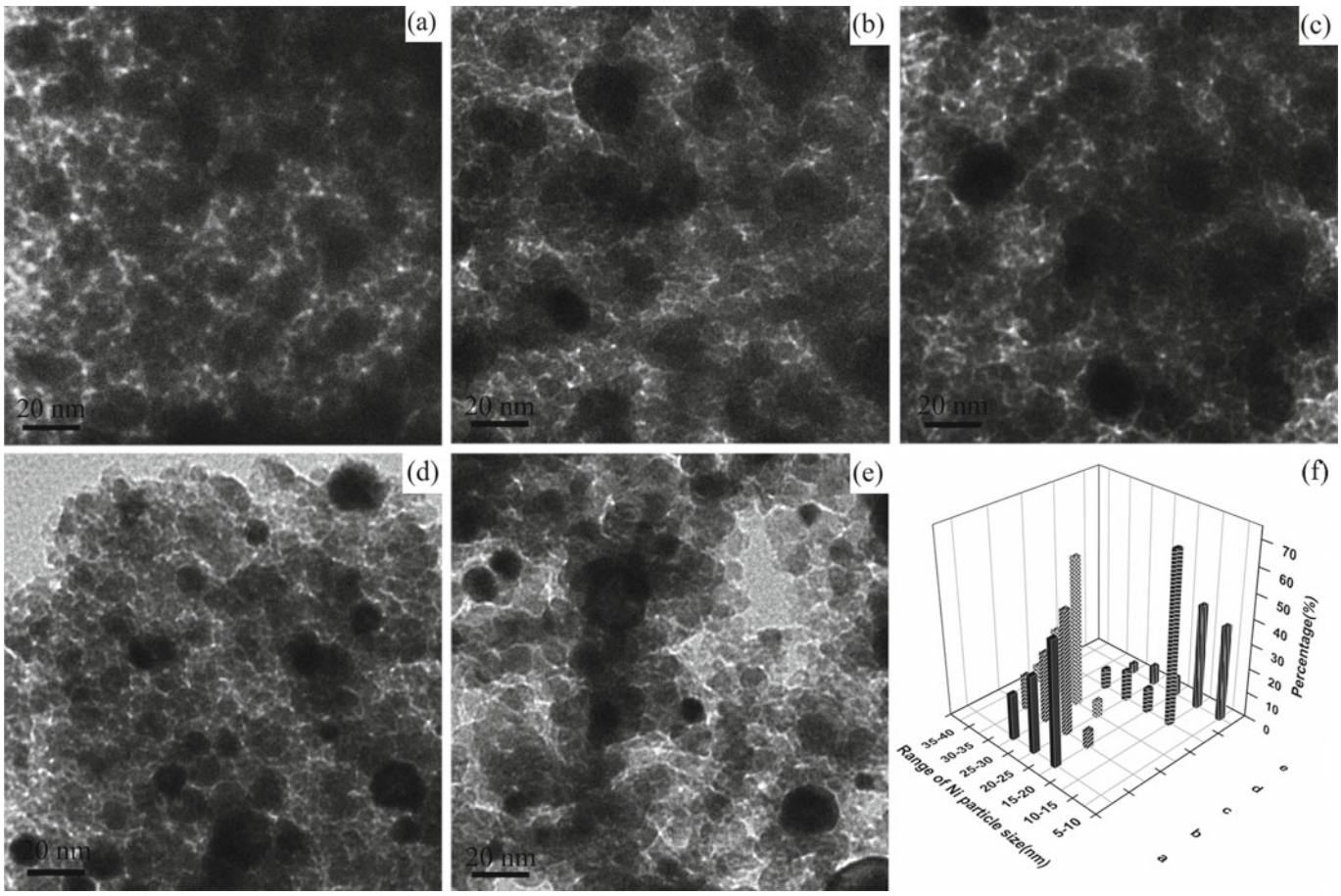

Figure 3. TEM micrographs of 30Ni-2E (a), 30Ni-5E (b), 30Ni-10E (c), 30Ni-2P (d), 30Ni-2G (e), and practical size distribution (f)

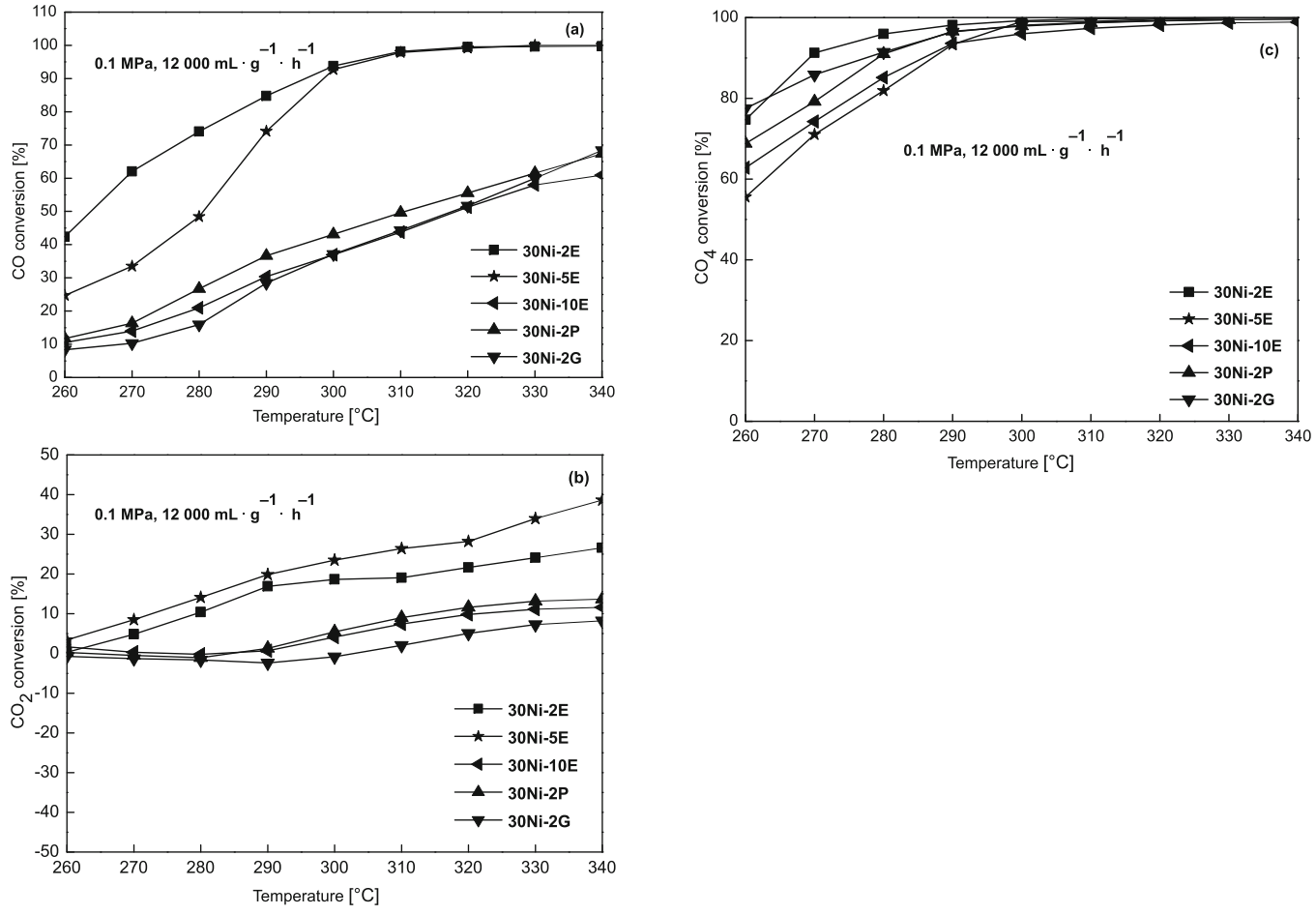

Figure 4. CO conversion (a), CO_2 conversion (b), and CH_4 selectivity (c)

low-temperature is a structure-sensitive reaction. Larger Ni particles have a lower surface area for CO conversion and thus exhibit a lower methanation rate, while smaller Ni particles have a larger surface area for CO conversion which is beneficial for a higher methanation rate. However, smaller Ni particles, having amounts of Ni step sizes, are easily covered by carbon resulting in

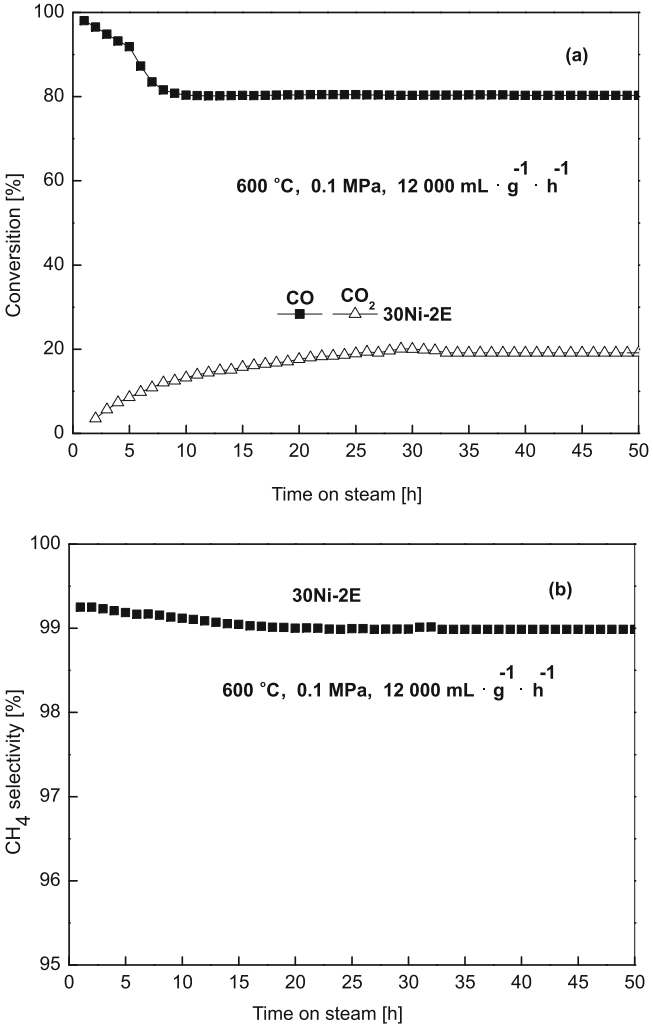

Figure 5. CO and CO_2 conversion (a), and CH_4 selectivity (b) for the stability test of 30Ni-2E

fast deactivation of Ni catalysts, and thus have a low methanation rate[23].

The stability test of 30Ni-2E, the optimal catalyst among the five Ni-based catalysts, is conducted at 600°C, 2 MPa and 12 000 mL · g^{-1} · h^{-1}. In order to suppress the formation of both encapsulating carbon and filamentous carbon during syngas methanation reaction, 30 mol% water vapor is added into the reaction system according to literature[24]. As shown in Figure 5a, with time on stream increase, the CO conversion of 30Ni-2E decreases gradually from 99.5 to 81.6%, while CO_2 conversion increases slowly to ~20%. Then the CO and CO_2 conversion almost remain unchanged. Figure 5b shows the CH_4 selectivity, which maintains ~99% during the whole life-time test. The good stability can be attributed to that Ni particles are scattered and spatially isolated by Al_2O_3, which can prevent the sintering of Ni particles. It proves 30Ni-2E catalyst not only has optimal catalytic activity at low-temperature, but also shows good stability at high-temperature.

CONCLUSIONS

Ni-Al_2O_3 catalysts prepared by SCM for syngas methanation are enhanced by adopting various heating rate (2°C · min^{-1}, 5°C · min^{-1} and 10°C · min^{-1}) and different solvent (ethanol, n-propanol and glycerol). Both heating rate and solvent have effects on Ni particle size, thus affecting the catalytic activity. 30Ni-2E prepared in ethanol at 2°C · min^{-1} exhibits better catalytic activity. In addition, the production rate of methane per unit mass of nickel is greatly influenced by Ni particle size. The maximum production rate of methane per unit mass of nickel can be achieved to 221 mmol · g^{-1} · h^{-1} on around 20.8 nm Ni particles (determined by XRD), at 280°C, 0.1 MPa and 12 000 mL · g^{-1} · h^{-1}.

ACKNOWLEDGMENT

This work is financially supported by the National Science and Technology Supporting Plan (2012AA050102).

LITERATURE CITED

1. Kopyscinski, J., Schildhauer, T.J. & Biollaz, S.M.A. (2010). Production of synthetic natural gas (SNG) from coal and dry biomass-A technology review form 1950 to 2009. Fuel. 89(8), 1763–1783. DOI: 10.1016/j.fuel.2010.01.027.

2. Gao, J.J., Wang, Y.L., Ping, Y., Hu, D.C., Xu, G.W., Gu, F.N. & Su, F.B. (2012). A thermodynamic analysis of methanation reactions of carbon oxides for the production of synthetic natural gas. RSC Adv. 2(6), 2358–2368. DOI: 10.1039/c2ra00632d.

3. Xavier, K.O., Sreekala, R., Rashid, K.K.A., Yusuf, K.K.M. & Sen, B. (1999). Doping effects of cerium oxide on Ni/Al_2O_3 catalysts for methanation. Catal. Today. 49(1–3), 17–21. DOI: 10.1016/S0920-5861(98)00403-9.

4. Derekaya, F.B. & Yasar, G. (2011). The CO methanation over NaY-zeolite supported Ni/Co_3O_4, Ni/ZrO_2, Co_3O_4/ ZrO_2 and Ni/Co_3O_4/ZrO_2 catalysts. Catal. Commun. 13(1), 73–77. DOI: 10.1016/j.catcom.2011.06.024.

5. Kopyscinski, J., Schildhauer, T.J. & Biollaz, S.M.A. (2011). Fluidized-Bed methanation: Interaction between kinetics and mass transfer. Ind. Eng. Chem. Res. 50(5), 2781–2790. DOI: 10.1021/ie100629k.

6. Duan, X.Z., Qian, G., Zhou, X.G., Sui, Z.J., Chen, D. & Yuan, W.K. (2011). Tuning the size and shape of Fe nanoparticles on carbon nanofibers for catalytic ammonia decomposition. Appl. Catal. B: Environ. 101(3–4), 189–196. DOI: 10.1016/j.apcatb.2010.09.017.

7. Utaka, T., Takeguchi, T., Kikuchi, R. & Eguchi, K. (2003). CO removal from reformed fuels over Cu and precious methal catalysts. Appl. Catal. A: Gen. 246(1), 117–124. DOI: 10.1016/S0926-860X(03)00048-6.

8. Vannice, M.A. (1975). The catalytic synthesis of hydrocarbons form H_2/CO mixtures over the group VIII methas: 1. The specific activities and product distributions of supported metals. J. Catal. 37(3), 449–461. DOI: 10.1016/00214-9517(75)90181-5.

9. Kim, S.H., Lee, W.D. & Lee, H.I. (2013). Effect of CeO_2 on CO removal over CeO_2-modified Ni catalyst in CO-rich syngas. Korean J. Chem. Eng. 30(4), 860–863. DOI: 10.1007/s11814-013-0007-x.

10. Wieslawa, C.B. (2013). Influence of the exchanged metal ions (Cu, Co, Ni and Mn) on the selective catalytic reduction of NO with hydrocarbons over modified ferrierite. Pol. J. Chem. Tech. 15(2), 10–15. DOI: 10.2478/pjct-2013-0018.

11. Shi, P. & Liu, C.J. (2009). Characterization of silica supported nickel catalyst for methanation with improved activity by room temperature plasma treatment. Catal. Lett. 133(1–2), 112–118. DOI: 10.1007/s10562-009-0163-0.

12. Zhao, A.M., Ying, W.Y., Zhang, H.T., Ma, H.F. & Fang, D.Y. (2012). Ni-Al_2O_3 catalysts prepared by solution combustion method for syngas methanation. Catal. Commun. 17, 34–38. DOI: 10.1016/j.catcom.2011.10.010.

13. Zhang, J., Xu, H.Y., Jin, X.L., Ge, Q.J. & Li, W.Z. (2005). Characterizations and activities of the nano-sized Ni/Al_2O_3 and Ni/La-Al_2O_3 catalysts for NH_3 decomposition. Appl. Catal. A: Gen. 290(1–2), 87–96. DOI: 10.1016/j.apcata.2005.05.020.

14. Guimon, C., Auroux, A., Romero, E. & Monzon, A. (2003). Acetylene hydrogenation over Ni-Si-Al mixed oxides prepared by sol-gel technique. Appl. Catal. A: Gen. 251(1), 199–214. DOI: 10.1016/S0926-860X(03)00318-1.

15. Zhang, Y.H., Xiong, G.X., Sheng, S.S., Liu, S.L. & Yang, W.S. (1999). Interaction of NiO with γ–Al_2O_3 supporter of NiO/γ-Al_2O_3 catalysts. Acta Phys. Chem. Sim. (Wuli Huaxue Xuebao) 15(8), 735–741. DOI: 10.3866/PKU.WHXB19990813.

16. Rynkowski, J.M., Paryjczak, T. & Lenik, M. (1993). On the nature of oxidic nickel phases in NiO/ γ–Al_2O_3 catalysts. Appl. Catal. A: Gen. 106(1), 73–82. DOI: 10.1016/0926-860X(93)80156-K.

17. Vos, B., Poels, E. & Bliek, A. (2001). Impact of calcination conditions on the structure of alumina-supported nickel particles. J. Catal. 198(1), 77–88. DOI: 10.1006/jcat.2000.3082.

18. Zou, X.J., Wang, X.G. & Li, L. (2010). Development of highly effective supported nickel catalysts for pre-reforming of liquefied petroleum gas under low steam to carbon molar ratios. Int. J. Hydrogen. Energ. 35(22), 12191–12200. DOI: 10.1016/j.ijhydene.2010.08.080.

19. Yang, J., Wang, X.G., Li, L., Shen, K., Lu, X.G. & Ding, W.Z. (2010). Catalytic conversion of tar from hot coke oven gas using 1-methylnaphthalene as a tar model compound. Appl. Catal. B: Environ. 96(1–2), 232–237. DOI: 10.1016/j.apcatb.2010.02.026.

20. Koo, K.Y., Roh, H.S., Seo, Y.T., Seo, D.J., Yoon, W.L. & Park, S.B. (2008). A highly effective and stable nano-sized Ni/MgO- Al_2O_3 catalyst for gas to liquids (GTL) process. Int. J. Hydrogen. Energ. 33(8), 2036–2043. DOI: 10.1016/j.ijhydene.2008.02.029.

21. Xin, Q. & Luo, M.F. (2009). Xian Dai Cui Hua Yan Jiu Fang Fa (1st ed). Beijing: Science Press.

22. Gao, J.J., Jia, C., Zhang, M.J., Gu, F., Xu, G.W. & Su, F.B. (2013). Effect of nickel nanoparticle size in Ni/α-Al_2O_3 on CO methanation reaction for the production of synthetic natural gas. Catal. Sci. Technol. 3(8), 2009–2015. DOI: 10.1039/C3CY00139C.

23. Chen, D., Christensen, K.O., Ochoa-Fernandez, E., Yu, Z.X., Totdal, B., Latorre, N., Monzon, A. & Holmen, A. (2005). Synthesis of carbon nanofibers: effects of Ni crystal size during decomposition. J. Catal. 229(1), 82–96. DOI: 10.1016/j.jcat.2004.10.017.

24. Jimeneza, V., Sancheza, P., Panagiotopouloub, P., Valverdea, J.L. & Romeroa, A. (2010). Methanation of CO, CO_2, and selective methanation of CO, in mixtures of CO and CO_2, over ruthenium carbon nanofibers catalysts. Appl. Catal. A: Gen. 390(1–2), 35–44. DOI: 10.1016/j.apcata.2010.09.026.